Supplementary Materials

S1. Reason for the lower strength of FG than CG

A lower tensile strength was measured in FG than CG, even though the microstructural scaling was substantially smaller in the former. This deviates from the generally accepted tendency in martensitic steels, where strength gently increases with a refinement of block size [9].

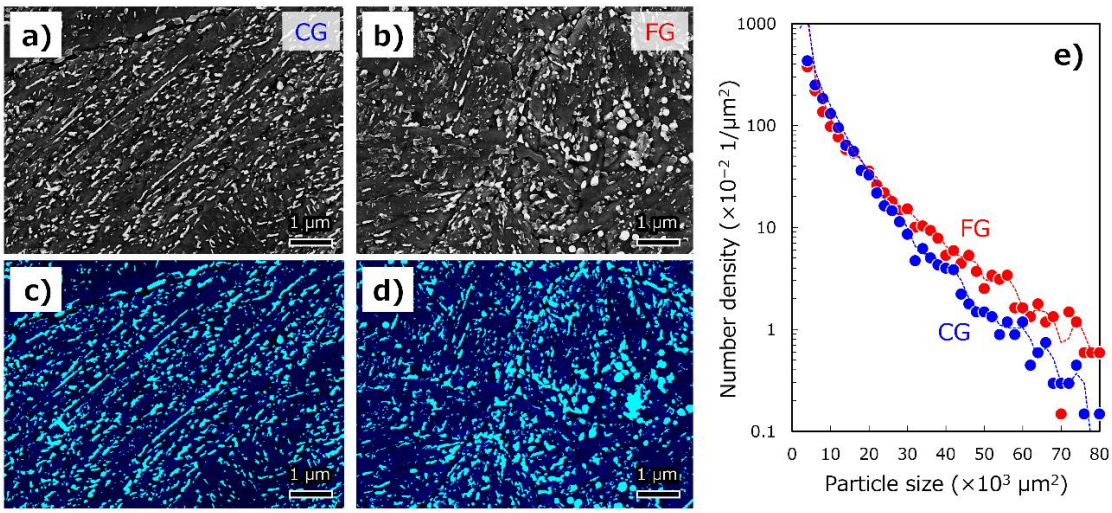

Fig. S1 (a)(b) SEM images of the microstructures in (a) CG and (b) FG after etched with picric acid, wherein cementite precipitates are appeared as white particles. The relevant bipolarized images are depicted in (c) and (d). (e) presents the number density histograms of particle sizes, constructed from the analysis of SEM images containing more than 20000 particles for each material.

In martensitic steels tempered at a relatively high temperature above 700 K, cementite or alloy carbides precipitations become another contributor to the strengthening in addition to fine lath martensitic microstructure [13]. Fig. S1 (a) and (b) show the microstructures of CG and FG after etching with picric acid, in which cementite is visualized as white particles. While the small dots or film-like cementite are finely dispersed inside as well as along boundaries of laths in CG, some coarse spherical particles with hundreds of nanometers are seen in FG. The areal number density of these cementite determined from the analysis of the images containing more than 20000 particles for each material (examples are presented in Fig. S1 (c) and (d)) are plotted in Fig. S1 (e) as a function of their sizes. Clearly, FG contained a greater number of large particles than CG. Given that the total volume fraction of cementite was fixed, the result indicates a coarser and more uneven distribution of cementite in the former. Such a coarse morphology of cementite might counteract the microstructure refinement effect, a plausible reason for the lower tensile strength of FG than CG, even though the underlying

rationale for this morphological difference is unclear. Probably, FG contained a higher fraction of retained austenite as the M_S temperature decreased with a reduction in PAG size, as demonstrated in [32]. Those retained austenite absorbed matrix carbon and then transformed into coarse cementite during the tempering process, producing the large spherical particles in Fig. S1 (b).

S2. The insignificance of crack deflection and closure effects

The winding pathway of the H-assisted crack, which was more extensive in coarser PAG material, shown in Fig. 4 (d)~(f) superficially invokes crack deflection or roughness-induced crack closure effects [44,45] as the causes of slower FCG rate in FG than MG and CG (Fig. 2 (a)). In general, both these factors diminish the effective stress intensity factor and thereby reduce the driving force to propel the crack-tip into purely mode I direction. In Fig. S2, the optical micrographs of the lateral CT specimen surfaces are displayed for the regions corresponding to ΔK = 15 MPa·m$^{1/2}$, nevertheless revealing the magnitude of crack deflection was substantial even in air for the materials with coarser PAG. If the crack deflection was a root cause of the inverse grain size-dependence observed at low ΔK, we cannot, on the other hand, explain the absence of any microstructural impacts on the FCG rate in air (Fig. 2 (a)).

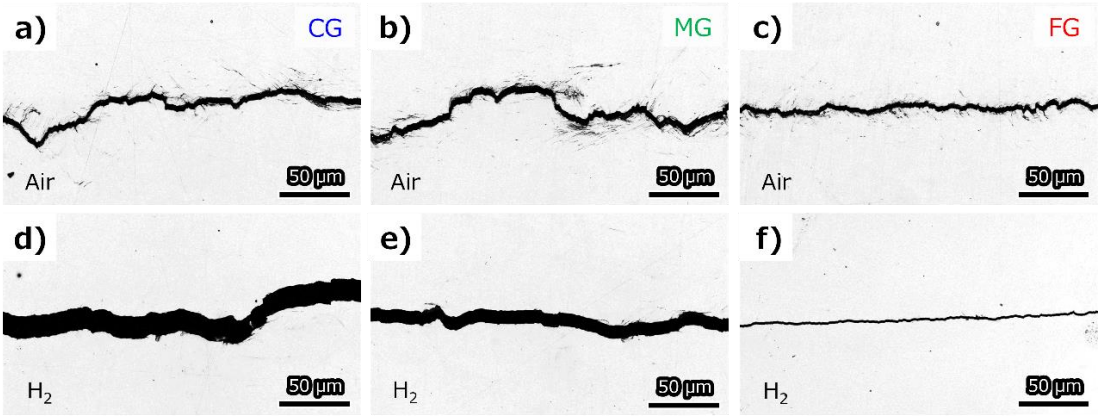

Fig. S2 Optical micrographs around the lateral surfaces of CT specimens of (a)(d) CG, (b)(e) MG, and (c)(f) FG in (a)~(c) air and (d)~(f) 90 MPa H_2 gas. The relevant ΔK is 15 MPa·m$^{1/2}$, and the crack growth direction is from left to right in each image.

The contribution of crack closure can be evaluated by substituting ΔK with the effective stress intensity factor range, ΔK_{eff}, where the load below the crack-opening point is subtracted in the ΔK calculation. Here, we used the experimentally measured relationship between applied load and crack mouth opening displacement during the FCG tests for the determination of the crack-opening point at each ΔK level. For the detailed methodology, the readers shall refer to [34].

The FCG rates assembled as the functions of ΔK and ΔK_{eff} are plotted in Fig. S3. All the data of FG, MG, and CG slightly shifted into the smaller side in abscissa when ΔK_{eff} was used, indicating that the crack closure more or less influenced on the FCG rates in H_2 gas. However, the comparative magnitude relationship between the three materials was still invariant. From this analysis, we can rule out the role of crack closure as the crack decelerator in coarser PAG materials. The abnormal grain size-dependence at the low ΔK situation might be an intrinsic effect of microstructural variation, as discussed in the main text.

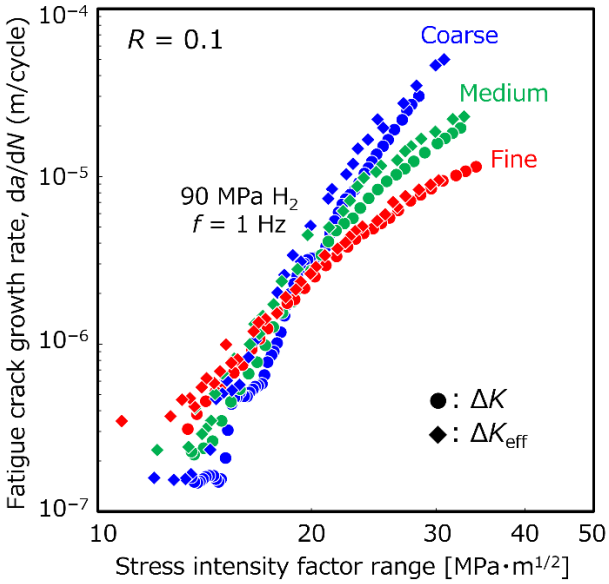

Fig. S3 Fatigue crack growth rates of CG, MG, and FG in 90 MPa H_2 gas assembled versus apparent stress intensity factor range, ΔK, and effective stress intensity factor range, ΔK_{eff}. For the determination method of ΔK_{eff}, the readers shall refer to [34].